dynamics of dissolved nutrient patches. We have yet to identify the frequency of occurrence and magnitude spectra of such patches in specific microbial food webs. They undoubtedly represent interesting ecological niches for bacteria, and they will also contribute much to our understanding of the flow of nutrients and energy in aquatic ecosystems if they prove to be major pathways.

References and notes

1. J. C. Goldman, *Bull. Mar. Sci.* **35**, 462 (1984).
2. E. M. Purcell, *Am. J. Phys.* **45**, 3 (1977).
3. G. A. Jackson, *Limnol. Oceanogr.* **32**, 1253 (1987).
4. W. Bell and R. Mitchell, *Biol. Bull.* **143**, 265 (1972).
5. J. G. Mitchell, A. Okubo, J. A. Fuhrman, *Nature* **316**, 58 (1985); J. D. Bowen, K. D. Stolzenbach, S. W. Chisholm, *Limnol. Oceanogr.* **38**, 36 (1993).
6. N. Blackburn, unpublished observations.
7. _____, F. Azam, Å. Hagström, *Limnol. Oceanogr.* **42**, 613 (1997).
8. Samples were taken, immediately before observation, from the vicinity of algal mats in a large seawater aquarium with high through-flow. The microbial community could be characterized as being rich and diverse. Identical communities have been observed in completely natural habitats. A standard microscope fitted with a dark-field condenser was used for observation with a 10× objective giving a depth of field of ~20 μm. The magnification was increased for some recordings with a magnifying lens. Samples were observed in a chamber made by a 1.5-mm-thick rubber O-ring placed on top of a microscope slide and covered with a cover slip. A fiber optic light source was used for illumination to minimize heat transfer. A standard video camera and VCR were used for recordings.
9. A. Andersson, C. Lee, F. Azam, Å. Hagström, *Mar. Ecol. Prog. Ser.* **23**, 99 (1985); P. A. Jumars, D. L. Penry, J. A. Baross, M. J. Perry, B. W. Frost, *Deep-Sea Res.* **36**, 483 (1989).
10. J. T. Lehman and D. Scavia, *Proc. Natl. Acad. Sci. U.S.A.* **79**, 5001 (1982).
11. P. J. L. Williams and L. R. Muir, in *Ecohydrodynamics*, J. C. J. Nihoul, Ed. (Elsevier, New York, 1981), pp. 209–218; D. J. Currie, *J. Plankton Res.* **6**, 591 (1984); G. A. Jackson, *Nature* **284**, 439 (1980).
12. D. A. Brown and H. C. Berg, *Proc. Natl. Acad. Sci. U.S.A.* **71**, 1388 (1974).
13. T. Fenchel, *Microbiology* **140**, 3109 (1994); J. G. Mitchell *et al.*, *Appl. Environ. Microbiol.* **61**, 877 (1995); J. G. Mitchell, L. Pearson, S. Dillon, K. Kantalis, *ibid.*, p. 4436; J. G. Mitchell, L. Pearson, S. Dillon, *ibid.* **62**, 3716 (1996); G. M. Barbara and J. G. Mitchell, *ibid.*, p. 3985.
14. Samples of seawater were enriched with 0.02% tryptic soy broth and left overnight, after which the culture contained strains of highly motile bacteria. Samples were sandwiched between a slide and cover slip after the addition of cells from a pure culture of *Pavlova lutheri*. A ring of bacteria around the air-water interface of the chamber indicated near anoxia inside the chamber.
15. P. A. Wheeler, in *Nitrogen in the Marine Environment*, E. J. Carpenter and D. G. Capone, Eds. (Academic Press, New York, 1983), p. 309.
16. F. Azam and J. W. Ammerman, in *Flows of Energy and Materials in Marine Ecosystems*, M. J. R. Fasham, Ed. (Plenum, New York, 1984), p. 345.
17. N. Blackburn, T. Fenchel, J. Mitchell, data not shown.
18. J. D. Bowen and K. D. Stolzenbach, *J. Fluid Mech.* **236**, 95 (1992).
19. L. Karp-Boss, E. Boss, P. A. Jumars, *Oceanogr. Mar. Biol. Annu. Rev.* **34**, 71 (1996).
20. H. C. Berg and D. A. Brown, *Nature* **239**, 500 (1972).
21. Video sequences were digitized to computer memory at 25 frames s^{-1}. The resulting digital film-strips were analyzed frame by frame for trajectories of movement by LabTrack (DiMedia, Kvistgaard, Denmark). Objects moving out of the plane of focus resulted in short tracks and were filtered out of the set of track vectors. Tumbles were detected at points where changes in trajectory angle between two video frames exceeded 1 rad. Runs were defined as periods between tumbles.
22. The enteric bacterium *E. coli* swims in straight runs interspersed by tumbles (*20*). Positive taxis is achieved by lengthening runs when positive changes in concentration are detected over a period of time (*12*). The model refined by Brown and Berg states that the mean increase in run duration $\Delta\tau$ is proportional to the positive rate of change of attractant concentration

$$\Delta\tau = \frac{\alpha}{K_D}\frac{\partial C}{\partial t}$$

where C is concentration, K_D is a dissociation constant (100 μM), and α is a sensitivity constant (1000 s). Simulations were performed by allowing cells to move against a concentration field (*3*). Cells were moved a distance determined by their swimming velocity and heading angle from a physical location whose attractant concentration was C_1 to another location of concentration C_2, within each simulated time step dt. The change in mean run duration could thus be calculated as

$$\Delta\tau = \frac{\alpha}{K_D}\frac{C_2 - C_1}{dt}$$

Negative changes were ignored. Run durations are Poisson distributed (*12*). The probability of tumbling after each time step is $dt/(\tau + \Delta\tau)$. The desired Poisson process was implemented with a random generator to decide whether or not to tumble after each time step. Tumbles were simulated as reversals, and a Brownian rotation of 1 rad s^{-1} was introduced. Swimming velocities and mean run durations were acquired from tracks of live cells.
23. The steady-state concentration field $C(r)$ was calculated as

$$C(r) = \frac{E}{4\pi D\sqrt{r}}$$

where oxygen exudation rate $E = 0.25$ fmol s^{-1} was estimated from light-saturated photosynthesis of a cell 4 μm in diameter. The diffusion coefficient $D = 10^{-5}$ cm^2 s^{-1}. The inverse square-root dependency on the distance r from the source was introduced instead of inverse proportionality (*3*) to more closely approximate its shape in the flat chamber.
24. The concentration field $C(r,t)$ of a spreading patch was calculated as

$$C(r,t) = M(4\pi rDt)^{-1.5}e^{-\frac{r^2}{4Dt}}$$

where M is the amount of matter released (1 pmol), and $D = 10^{-5}$ cm^2 s^{-1}. Simulations were based on 100 individuals initially distributed randomly within a radius of 1 mm from the source. Velocity $v = 50$ μm s^{-1}, $\tau = 0.4$ s.
25. The mass flow of a solute at concentration C with diffusion coefficient D toward a sphere of radius a is $4\pi aDC$.

26. We thank the Swedish Foundation for International Cooperation in Research and Higher Education (STINT), the Danish National Research Council (SNF), the Australian Research Council, and Flinders University for support of this study.

12 June 1998; accepted 3 November 1998

Prevention of Population Cycles by Parasite Removal

Peter J. Hudson,* Andy P. Dobson, Dave Newborn

The regular cyclic fluctuations in vertebrate numbers have intrigued scientists for more than 70 years, and yet the cause of such cycles has not been clearly demonstrated. Red grouse populations in Britain exhibit cyclic fluctuations in abundance, with periodic crashes. The hypothesis that these fluctuations are caused by the impact of a nematode parasite on host fecundity was tested by experimentally reducing parasite burdens in grouse. Treatment of the grouse population prevented population crashes, demonstrating that parasites were the cause of the cyclic fluctuations.

Mathematical models have shown that a density-dependent response acting with a time delay can generate population cycles between natural enemies and their prey (*1*). Indeed, trophic interactions rather than intrinsic mechanisms are now considered by many to be the principal cause of cycles in microtine rodents (*2*), snowshoe hares (*3*), and red grouse (*4*). The definitive test of these hypotheses is to stop population cycles by manipulating the causative mechanism. Here, we report on a long-term, large-scale, replicated field experiment that examined the capacity of parasites to cause cycles. The impact of the parasitic nematode *Trichostrongylus tenuis* on individual red grouse (*Lagopus lagopus scoticus*) was reduced through the application of an anthelmintic before a cyclic population crash in northern England.

Extensive investigations of hunting records from 175 individually managed grouse populations, coupled with detailed intensive demographic studies, have shown that 77% of red grouse populations exhibit significant cyclic fluctuations with a period between 4 and 8 years (Fig. 1A) (*4*). Population growth rate is negatively related to the intensity of worm infection in adult grouse (Fig. 1B), and poor breeding production is correlated with worm intensity (Fig. 1C), so that population crashes are associated with high parasite intensities. Analyses of parasite-host models predict that parasitic helminths can cause population cycles when they induce a reduction in host fecundity

P. J. Hudson, Institute of Biological Sciences, University of Stirling, Stirling FK9 4LA, UK. A. P. Dobson, Department of Ecology and Evolutionary Biology, Eno Hall, Princeton University, Princeton, NJ 08544–1003, USA. D. Newborn, Game Conservancy Trust, Swaledale, North Yorkshire DL8 3HG, UK.

*To whom correspondence should be addressed. E-mail: p.j.hudson@stir.ac.uk

that is large in relation to the impact of the parasite on host survival (*5*), and experimental studies have demonstrated that poor breeding in female grouse is caused by the nematode *Trichostrongylus tenuis* (*6*). Extensive demographic studies have shown a clear relation between bag records and count data (*4*), although hunters tend to stop shooting when autumn densities are <30 birds km^{-2} (Fig. 1A). Bag records are not influenced by any hunting restrictions, and in this system they provide a reasonable index of abundance and a very good qualitative description of the observed periodic crashes.

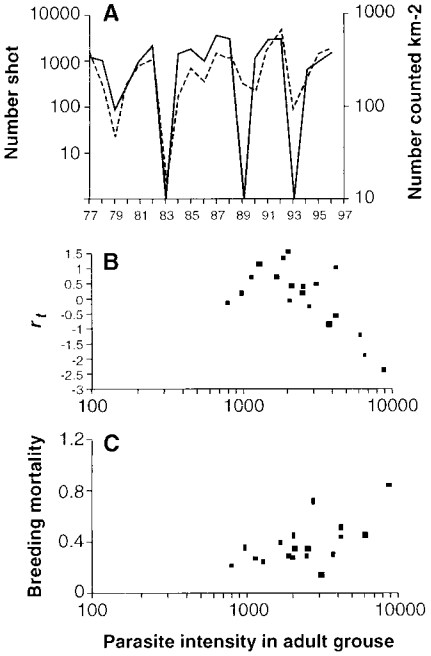

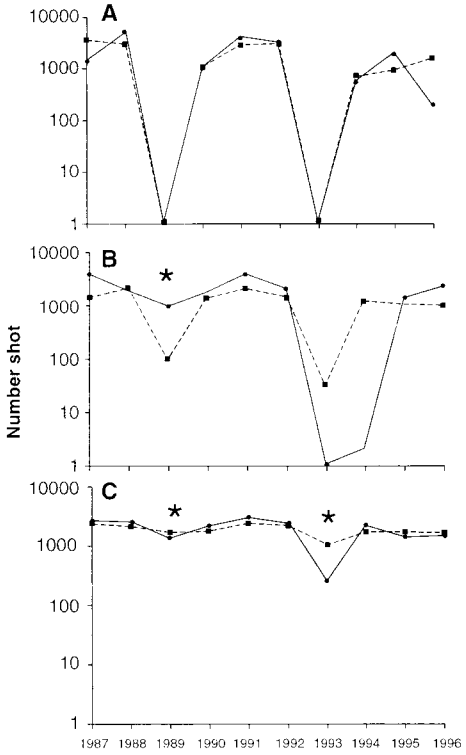

Fig. 1. (**left**) Population dynamics of red grouse as illustrated from the detailed studies on one population in northern England. (**A**) Numbers of red grouse shot (solid line) and numbers counted per square kilometer (dashed line) before harvesting. (**B**) Plot of annual population growth rate [r_t = (ln N_{t+1} − ln N_t)] against mean log worm intensity in breeding adult grouse (r = −0.676; 95% bootstrap confidence limits 0.901 to 0.216). (**C**) Plot of breeding mortality [log maximum clutch size (12) − log mean brood size at 6 weeks] against mean log worm intensity (r = 0.641; 95% bootstrap confidence limits 0.287 to 0.816). **Fig. 2.** (**right**) Population changes of red grouse, as represented through bag records in (**A**) the two control sites, (**B**) the two populations with a single treatment each, and (**C**) the two populations with two treatments each. Asterisks represent the years of treatment when worm burdens in adult grouse were reduced.

Table 1. Population parameters for *T. tenuis* and red grouse. The derivation of the parameter estimates is discussed elsewhere (*4*–*6*). NA, not applicable.

Parameter	Symbol	Estimated value	Range
Grouse fecundity (year^{-1})	a	1.8	0–2
Grouse mortality (year^{-1})	b	1.05	NA
Parasite fecundity (year^{-1})	λ	11	9.2–11.5
Adult worm mortality (year^{-1})	μ	1.0	0.8–1.2
Mortality of free-living stages (year^{-1})	γ	6.5–13	NA
Parasite pathogenicity (worm^{-1} year^{-1})	α	3×10^{-4}	NA
Parasite reduction in host fecundity (worm^{-1} year^{-1})	δ	5×10^{-4}	NA
Aggregation of parasites in host	k	1.0	0.5–1.8
Density-dependent reduction in grouse fecundity and survival	Δ	0.004	NA
Increase in worm mortality in treated birds	c	52 (life expectancy, 1 week)	NA
Transmission rate (larvae^{-1} host^{-1} year^{-1})	β	0.11	0.06–0.15

Long-term data from six independently managed grouse moors were used to predict cyclic crashes in grouse numbers in 1989 and again in 1993. In 1989, we worked with keepers and caught and orally treated grouse with the anthelmintic Levamisole hydrochloride in four of these six populations. In 1993, this was repeated on two of the populations, providing data from a total of six populations—two that had been treated to stop two population crashes, two that had been treated to stop one population crash, and two untreated control populations. During each treatment year, grouse were caught at night in early spring when most of the birds had formed mating pairs. Birds were dazzled with a strong quartz-halogen lamp while roosting, caught in a net, and treated with Levamisole hydrochloride. Each bird was marked with a reflective tag that could be seen on subsequent catching nights. It was possible for a team of two people to catch and treat more than 100 birds in a single night. Radio tagging and subsequent monitoring showed that tagged and treated birds remained on their territories and had improved breeding. Birds were caught at random from accessible parts of the grouse habitat. Females were caught in preference to males to ensure the greatest impact of parasite removal on breeding production. Catching and treatment continued from when the snow melted to when females began laying eggs. Overall, between 1000 and 3000 grouse were caught and treated from each population. Depending on the size of each grouse population, our estimates showed that we treated between 15 and 50% of the adult breeding population. A sample of treated birds was shot from each population, and the intensities of worm infection were compared with those of untreated birds to confirm that treatment reduced the worm burdens. The numbers of harvested grouse were recorded during the subsequent hunting season.

In each of the six treatments, the application of Levamisole hydrochloride reduced the tendency of the population to exhibit cyclic

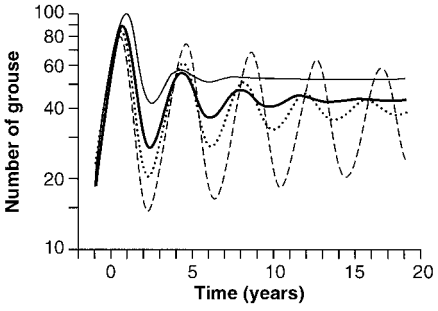

Fig. 3. The influence of treatment on the cycling of grouse populations. Changes in the number of grouse are shown in relation to the proportion of grouse treated. No treatment, dashed line; 5%, dotted line; 10%, thick solid line; and 20%, thin solid line.

population crashes (*7*). Reducing the parasite burdens reduced the variance in the population growth rate and produced an apparent reduction in the decline of the treated populations (Fig. 2). This experiment illustrated that parasitic nematodes were necessary for the cyclic declines in abundance that were observed in grouse populations. In both populations that were treated twice (Fig. 2C) and in one of the populations that was treated once (Fig. 2B), the effect of the treatment was apparent in comparison with the controls, although the results are less clear in the remaining population, which was treated just once. We suspect this was because the keeper treated a relatively low proportion of the grouse population (~15%). Even with these results, the findings were still significant and demonstrate that parasites played a key role in causing population cycles.

To determine the effectiveness of the treatment, we calculated the proportion of the population that should be treated in order to prevent a population crash. We addressed this problem with a modified form of the general macroparasite model (*5*) that incorporates the experimental procedures of direct oral treatment (*8*) (Table 1). Individuals in the model were classified as either untreated (with natural levels of infection) or treated (with no parasites). Treatment of a proportion (p) of the population was triggered in the model whenever the growth rate of the parasite population increased (becomes positive). The worms in the treated grouse suffered an increased mortality rate, so their life expectancy was <1 week, whereas the remaining untreated birds ($1 - p$) continued to release infective stages into the environment, which infected both treated and untreated hosts. Numerical solutions of the model's dynamics showed that treatment of >20% of the hosts was sufficient to prevent the cyclic crashes in host density (Fig. 3) and provided a good explanation for all the results of the experiment.

The results from this study show that population cycles in red grouse are the result of a single trophic interaction between a parasite and its host. Combined with the modified macroparasite model, these results show that parasites were both sufficient and necessary in causing cycles in these populations. They also show that intrinsic mechanisms do not need to be evoked as a cause of cyclic fluctuations in grouse abundance (*9*). Previous studies have undertaken detailed experiments at a lower spatial scale. For example, a factorial manipulation of the food and predators of snowshoe hares on 1-km^2 plots indicated that at least three trophic levels of interaction are involved in producing cycles (*3*). Nevertheless, to the best of our knowledge, this is the first time that manipulations of a mechanism in a cyclic species have demonstrated the cause of population cycles on a large scale.

References and Notes

1. R. M. May, *Complexity and Stability of Model Ecosystems* (Princeton Univ. Press, Princeton, NJ, 1973).
2. I. Hanski, P. Turchin, E. Korpimäki, H. Henttonen, *Nature* **364**, 232 (1993).
3. C. J. Krebs *et al.*, *Science* **269**, 1112 (1995).
4. P. J. Hudson, A. P. Dobson, D. Newborn, in *Ecology and Genetics of Host-Parasite Interactions*, D. Rollinson and R. M. Anderson, Eds. (Academic Press, London, 1985), pp. 77–89; P. J. Hudson, *Grouse in Space and Time* (Game Conservancy Trust, Fordingbridge, UK, 1992); G. R. Potts, S. C. Tapper, P. J. Hudson, *J. Anim. Ecol.* **55**, 21 (1986).
5. A. P. Dobson and P. J. Hudson, *J. Anim. Ecol.* **61**, 487 (1992); R. M. May and R. M. Anderson, *ibid.* **47**, 249 (1978).
6. P. J. Hudson, *ibid.* **55**, 85 (1986); _____, D. Newborn, A. P. Dobson, *ibid.* **61**, 477 (1992).
7. Variance in the rate of population change ($\ln N_{t+1} - \ln N_t$) was significantly greater in control populations than in populations that were treated once ($F = 2.74$, $P < 0.05$) and in populations that were treated twice ($F = 36.5$, $P < 0.001$), but there was no difference between control populations ($F = 1.07$, $P > 0.2$).
8. The dynamics of the parasitic nematode and the grouse were modeled with six coupled differential equations. These describe changes in treated hosts (H_T), untreated hosts (H_U), the adult parasite population in these two classes of host (P_T and P_U, respectively), the free-living stages of the parasite (eggs and larvae) (W), and the chicks produced by the hosts (C). The parameter values and definitions are given in Table 1.

$$dH_U/dt = (1-p)\theta C - [b + \Delta(H_U + H_T)]H_U - \alpha P_U \quad (1)$$

$$dC/dt = a(H_U + H_T) - \delta(P_U + P_T) - (b + \theta)C \quad (2)$$

$$dP_T/dt = \beta H_T W - \{[\mathrm{if}(dP/dt)>0,\mu,c,\mu] + b + \alpha\} - \alpha \frac{P_T^2}{H_T}\frac{k+1}{k} \quad (3)$$

$$dP_U/dt = \beta H_U W - (\mu + b + \alpha)P_U - \alpha \frac{P_U^2}{H_U}\frac{k+1}{k} \quad (4)$$

$$dW/dt = \lambda(P_U + P_T) - [\gamma + \beta(H_U + H_T)]W \quad (5)$$

$$dH_T/dt = p\theta C - [b + \Delta(H_U + H_T)]H_T - \alpha P_T \quad (6)$$

9. R. Moss and A. Watson, *Ibis* **133** (suppl.), 113 (1991).
10. We thank the keepers and estates for their assistance; D. Tompkins, K. Wilson, and T. Benton for providing helpful comments on the manuscript; and D. Potts for his support throughout our studies on grouse.

13 August 1998; accepted 3 November 1998

Interleukin-13: Central Mediator of Allergic Asthma

Marsha Wills-Karp,* Jackie Luyimbazi, Xueying Xu, Brian Schofield, Tamlyn Y. Neben, Christopher L. Karp, Debra D. Donaldson

The worldwide incidence, morbidity, and mortality of allergic asthma are increasing. The pathophysiological features of allergic asthma are thought to result from the aberrant expansion of CD4$^+$ T cells producing the type 2 cytokines interleukin-4 (IL-4) and IL-5, although a necessary role for these cytokines in allergic asthma has not been demonstrable. The type 2 cytokine IL-13, which shares a receptor component and signaling pathways with IL-4, was found to be necessary and sufficient for the expression of allergic asthma. IL-13 induces the pathophysiological features of asthma in a manner that is independent of immunoglobulin E and eosinophils. Thus, IL-13 is critical to allergen-induced asthma but operates through mechanisms other than those that are classically implicated in allergic responses.

Recent decades have brought dramatic increases in the prevalence and severity of allergic asthma. In the United States, 15 million people are currently thought to suffer from the disorder (*1*). Allergic asthma is characterized by airway hyperresponsiveness (AHR) to a variety of specific and nonspecific stimuli, chronic pulmonary eosinophilia, elevated serum immunoglobulin E (IgE), and excessive airway mucus production (*2*). The pathophysiology of asthma is thought to be mediated by CD4$^+$ T lymphocytes producing a type 2 cytokine profile: (i) CD4$^+$ T cells are necessary for the induction of allergic asthma in murine models; (ii) CD4$^+$ T cells producing type 2 cytokines undergo expansion in these models and in patients with allergic asthma; and (iii) the amount of type 2 cytokines is increased in the airway tissues of asthmatics and animal models (*3*–*5*). The circumstantial evidence for the importance of IL-4 and IL-5, which are paradigmatic type 2 cytokines, has been compelling (*6*–*8*). However, although an antibody-mediated blockade of IL-4 during allergen sensitization ablates the development of allergic asthma, a similar blockade of IL-4 before or during an antigen challenge inhibits neither allergic in-

M. Wills-Karp, J. Luyimbazi, X. Xu, B. Schofield, Department of Environmental Health Sciences, Johns Hopkins University School of Hygiene and Public Health, Baltimore, MD 21205, USA. T. Y. Neben and D. D. Donaldson, Immunology Department, Genetics Institute, Cambridge, MA 02140, USA. C. L. Karp, Department of Medicine, Johns Hopkins University School of Medicine, Baltimore, MD 21205, USA, and Department of Molecular Microbiology and Immunology, Johns Hopkins University School of Hygiene and Public Health, Baltimore, MD 21205, USA.

*To whom correspondence should be addressed. E-mail: mkarp@welchlink.welch.jhu.edu